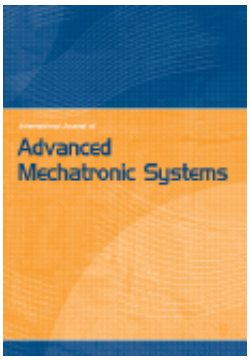

International Journal of Advanced Mechatronic Systems

ISSN online: 1756-8420 - ISSN print: 1756-8412
https://www.inderscience.com/ijamechs

An automatic artificial pancreas based on AOA-VPTIDF control algorithm

Akshaya Kumar Patra, Girija Sankar Panigrahi, Anuja Nanda

DOI: 10.1504/IJAMECHS.2023.10050454

Article History:

Received:	26 April 2022
Accepted:	03 August 2022
Published online:	09 January 2023

An automatic artificial pancreas based on AOA-VPTIDF control algorithm

Akshaya Kumar Patra*, Girija Sankar Panigrahi and Anuja Nanda

Department of Electrical and Electronics Engineering,
ITER,
Siksha 'O'Anusandhan University,
Bhubaneswar – 751030, Odisha, India
Email: akshayapatra@soa.ac.in
Email: hiakp@yahoo.com
Email: girijapanigrahi45@gmail.com
Email: anuja.sus@gmail.com
*Corresponding author

Abstract: The design of an Archimedes optimisation algorithm-variable parameter tilt integral derivative with filter (AOA-VPTIDF) controller for injecting the optimal dose of insulin through the artificial pancreases (APs) for blood glucose (BG) regulation in type I diabetes mellitus (TIDM) patients is presented in this manuscript. The AOA technique is used to optimise the controller parameters for better control execution in this strategy. MATLAB and Simulink are used to evaluate the AOA-VPTIDF controller's productivity in terms of accuracy, robustness and stability. The obtained results show that the AOA-VPTIDF controller is more effective at keeping blood sugar levels in the normal range (70–120 mg/dl). The relative result analysis with other well-known control techniques reveals the reason of improved control execution of the proposed controller.

Keywords: pancreas; insulin; blood; AOA-VPTIDF controller; diabetes.

Reference to this paper should be made as follows: Patra, A.K., Panigrahi, G.S. and Nanda, A. (2023) 'An automatic artificial pancreas based on AOA-VPTIDF control algorithm', *Int. J. Advanced Mechatronic Systems*, Vol. 10, No. 1, pp.21–32.

Biographical notes: Akshaya Kumar Patra is presently working as an Associate Professor in the Department of Electrical and Electronics Engineering, Institute of Technical Education & Research (ITER), Siksha 'O' Anusandhan University, Bhubaneswar, India. He received his PhD degree in Biomedical Engineering from Siksha 'O' Anusandhan University, Bhubaneswar, Odisha, India, in 2018. His main research includes control systems, robust control and biomedical engineering.

Girija Sankar Panigrahi is presently working as a research scholar in the Department of EE, ITER, S'O'A deemed to be University, Bhubaneswar, Odisha, India. He received his MTech degree from 'SOA' University, Bhubaneswar, Odisha, India, in 2011. His main research includes control systems, robust control, biomedical engineering, and image processing.

Anuja Nanda is presently working as an Assistant Professor in the Department of EEE, Institute of Technical Education & Research (ITER), Siksha 'O'Anusandhan University, Bhubaneswar, India. She received her M. Tech degree from 'SOA' University, Odisha, India, in 2009. Her main research includes control systems, and image processing.

1 Introduction

Diabetes mellitus, which is caused by the pancreas malfunctioning, is one of the most common illnesses, according to the World Health Organization (WHO). It affects the *normo-glycaemic* range of BG level in a human being by reducing insulin sensitivity. Several researchers are now working on a number of initiatives to solve this problem by developing modern medical equipment such as an automated micro-insulin dispenser (MID). The BG level has been manually managed since the open loop control approach was implemented. Due to challenges in managing internal system changes and external disruptions by using the control loop approach, hypoglycemic or hyperglycemic situations may develop. The development of implanted artificial pancreas (AP) that allows for an adequate dosage of insulin administration proportional to sensor measurements in patient's body might open the way for a closed loop control method to be implemented. A closed loop TIDM patient structure integrated with AP is depicted

in Figure 1. The AP is made up of three components: a sensor, a controller and a MID. The glucose sensor monitors the patient model's blood sugar levels and sends the data to the controller. With the information from the sensor the controller generates a control signal. According to the control signal, the MID pumps the desired quantity of insulin.

Figure 1 Overall graphical demonstration of TIDM patient with AP (see online version for colours)

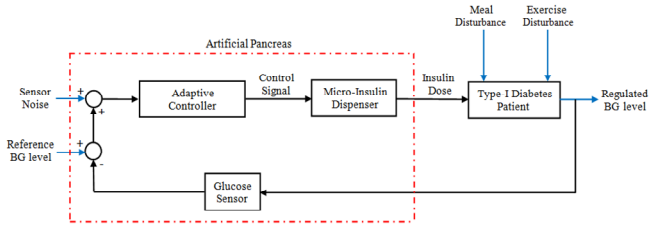

A variety of hurdles and constraints must be overcome in order to construct an ideal solution for the AP, including the impact of nonlinear characteristics, time-varying dynamics, different sources of interference, uncertainty, and lack of sensitivity to glucose are all factors to consider. Significant delay in glucose measurement, delayed post-infusion insulin absorption, endogenous insulin action, detection and evaluation of food intake, fluctuations in model parameters, asymmetric risk of extreme BG fluctuations, and time-based control requirements are all examples of control challenges (Chee and Fernando, 2003; Kamath and George, 2009). Despite significant technological advancement and development on the aforementioned issue, the control algorithm still needs to be improved significantly. Many authors recommended the PID controller as a feasible approach for assessing glucose excursions following insulin dosage adjustments in AP (Frederick and Tyrone, 2003; Sutradhar and Chaudhuri, 2002; Patra, 2020a, 2020b). The required performance insuring high accuracy, reliability and robustness could not be accomplished owing to glucose sensing time delay, insulin action, and non-variable gain parameters. Some of the optimal control techniques to deal with glucose monitoring issues include fuzzy control (Ibbini, 2006; Patra, 2020c), sliding mode (SM) control (Rmileh and Gabin, 2012; Gallardo and Ana, 2013; Patra, 2017a, 2018a), linear quadratic Gaussian (LQG) control (Patra, 2015, 2020e), H_∞ control (Chee and Andrey, 2005; Karimpour, 2012; Patra, 2014), and model predictive (MP) control (Patra, 2017b, 2018b), In comparison to PID controllers, glucose monitoring in patients within the *normo-glycaemia* range using the abovementioned controllers improved performance to some extent. Despite their improved performance these controllers are not totally immune to model disturbances and uncertainty. As a result, for improved performance and to avoid slow reaction after a meal disturbance, the current study proposes an alternative unique approach based on the Archimedes optimisation algorithm-variable parameter tilt integral derivative with filter (AOA-VPTIDF) controller.

The controller settings are modified for improved control execution in this suggested approach (AOA-VPTIDF) using the AO technique. The AOA-VPTIDF controller provides a wide range of control options for system parameters. The suggested controller adapts to all conceivable disturbances and patient situations in order to preserve patient *normo-glycemia*. When compared to other contemporary well-accepted strategies for controlling BG levels in TIDM patients, the proposed strategy ensures a more robust controller under both matched and mismatched uncertainty. The proposed patient model along with AOA-VPTIDF controller provides the noteworthy contributions which are summarised below.

- Development of numerical expressions of the glucose metabolism (GM) process in patient for glucose monitoring.
- To design a novel control strategy (AOA-VPTIDF) for patient model to monitor the BG level to attain the *normo-glycaemia*.
- Investigation of the patient activities with AOA-VPTIDF controller under the abnormal environments to justify its better performance.
- Comparative analysis is performed to certify superiority of the proposed approach.

The remaining of the manuscript is prearranged in the following order. The numerical clarifications of the GM process are shown in Section 2. Section 3 depicts the details about the proposed control strategy (AOA-VPTIDF) for maintaining normal BG levels. Section 4 displays the AOA-VPTIDF controller's numerical and simulation outputs. The concluding observations are shown in Section 5.

2 Problem formulation

2.1 Clinical support

Diabetes mellitus often known as *hyper-glycemia*, is a collection of clinical illnesses defined by a prolonged high level of AG exceeding 144 mg/dl. It can be caused by a shortage of insulin, its action or both. Diabetes is caused by the body's inability to properly utilise glucose. The dose of insulin in case of body determines whether it is types I or II. In type I diabetes, the patient's system is wholly unsuitable to make insulin. Insulin is administered at a slower rate and its action is limited in type II. Despite the fluctuating demands of food, fasting and exercise, glucose is properly monitored in the body (Barger and Rodbard, 1989; Chee and Fernando, 2003; Gallardo and Ana, 2013).

Glucose is the original energy source. For all of life's processes the human body need glucose. The venous blood (VB) takes glucose from the gastrointestinal compartment and absorbs it. The carbohydrate diet provides glucose to the gut compartment. It is the circulating glucose's 'external' source. The VB collects glucose from the intestine and subsequently transfers it to the liver. When the BG level falls too low, it is stored inside liver as glycogen and transported back into VB. It is the 'internal' glucose

supply. Inside the cell, glucose is metabolised with oxygen to produce energy, carbon dioxide, and water (Barger and Rodbard, 1989; Chee and Fernando, 2003; Gallardo and Ana, 2013).

The β cells in the pancreas produce insulin which regulates blood glucose (BG) levels. Insulin serves two major functions in a typical human with a high BG level: first, it allows the liver to absorb glucose and store it in the form of glycogen, which is especially important during meal intake. As a result, the liver and muscles can no longer produce excess 'internal' glucose. Second, insulin facilitates glucose absorption in the muscles and satisfies the body's peripheral energy requirements (Barger and Rodbard, 1989; Chee and Fernando, 2003; Gallardo and Ana, 2013). Both of the actions are observed to be impaired partially or totally in diabetic individuals due to abnormalities in metabolic process dynamics. When a diabetic patient's cells stop utilising glucose and the liver produces internal glucose, an uncontrolled BG level is observed. When the BG level exceeds the renal threshold glucose (RTG) of 162 mg/dl, the excess VB glucose is excreted through the kidney (Barger and Rodbard, 1989).

2.2 *Structure of patient*

The authors have provided many models that explain the mechanism of the GM process for glucose control as shown by glucose-insulin (GI) dynamics during the last few decades. Because of its structural simplicity and near approximation to human metabolic dynamics, Lehmann (1992, 1998) created a model that is commonly used in modelling and testing of a variety of control strategies. This model was used to test the effectiveness of the suggested controller for controlling glucose levels in the current investigation. Figure 2(a) depicts a GM process with AP, which consist of with six compartments including the peripheral, liver, kidney, stomach, heart and brain.

In the current study, this model was utilised to examine the effectiveness of the recommended controller for managing BG levels. Figure 2(a) shows a model of the GI interaction process with an integrated insulin dose controller, which has six parts: peripheral, liver, kidney, stomach, heart, and brain. Hepatic glucose production and intestinal absorption both result in glucose entering the bloodstream. Continuous monitoring of the AG is necessary to provide feedback to the AP. Every five minutes, the input to the AP is calculated, just like the insulin given into the VB by the implanted MID. The sensor technology and the support device utilised, on the other hand, decide the sample interval. Meal and exercise are presented as disruptions to the stomach and the periphery, respectively, in this model. After analysing insulin, glucose flow, and their features, the synthesis of the entire GM process in a diabetic patient is completed. Based on the action of insulin and glucose, a reduced model of the process of GM of the TIDM patient is presented in Figure 2(b). The transport of glucose flow directions is represented by solid arrow marks. The glucose transport promotion and inhibition with the help of insulin is indicated by +1 and –1 respectively.

Figure 2 (a) Compartmental model of GM process (b) The GI interaction in structure of patient (see online version for colours)

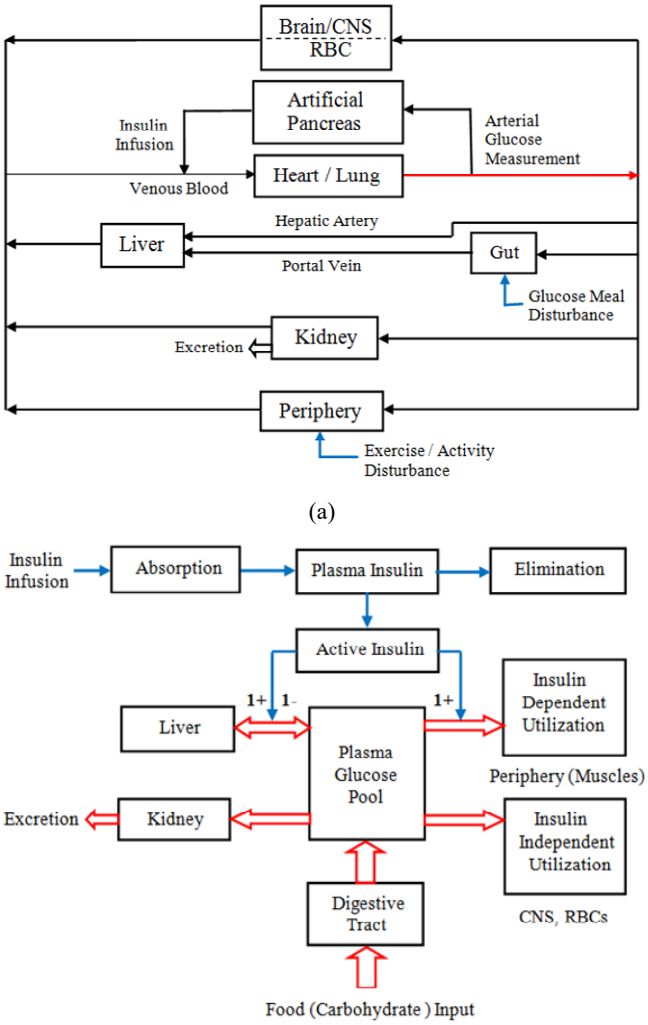

2.2.1 *Action of insulin*

The AP pumps optimum dose of insulin into the VB stream while the BG level increases. The insulin action inside the VB is stated as (Lehmann, 1992, 1998):

$$\frac{dI_p(t)}{dt} = \frac{I_{abs}(t)}{V_I} - K_e I_p(t) \tag{1}$$

where $I_p(t)$ is the plasma insulin level, $I_{abs}(t)$ is the insulin absorption rate of the VB, K_e is the constant of insulin elimination rate, and V_I is the volume of insulin distribution. The value of K_e and V_I are assumed as 0.123 min^{-1} and 99.4 dl separately. The differentiation of the active insulin concentration $I_a(t)$ (mU/dl) in the VB is stated as (Lehmann, 1992, 1998):

$$\frac{dI_a(t)}{dt} = K_1 I_p(t) - K_2 I_a(t) \tag{2}$$

where K_1 is the time delay rate constant of insulin action for $I_p(t)$, and K_2 is the time delay rate constant of insulin action for $I_a(t)$. The value of K_1 and K_2 are assumed as 0.00042 min^{-1} and 0.021 min^{-1} separately. The concentration of effective active insulin $I_{ea}(t)$, and concentration of effective plasma insulin $I_{ep}(t)$ in the VB are stated in the equations (3) and (4) respectively (Lehmann, 1992, 1998).

$$I_{ea}(t) = S_p\left(K_2/K_1\right) I_a(t) \tag{3}$$

$$I_{ep}(t) = \left(S_h/I_{basal}\right) I_p(t) \tag{4}$$

where S_p and S_h are the insulin sensitivity of peripheral and hepatic respectively. The range of ideal values of both insulin sensitivities (S_p and S_h) are taken as from 0 to 1.0. The I_{basal} denotes as the concentration of basal insulin, and its value is 1.0 mU/dl. The dynamic conditions of whole insulin activities in the GM process are communicated as in equations (1)–(4).

2.2.2 The profile of glucose in the digestive system

The glucose formation rate of the gastric emptying subsystem (GES) is known as gastric emptying rate $G_{empt}(t)$, and it is displayed in the Figures 3(a) and 3(b). The $G_{empt}(t)$ rises up to the maximum value $V\max_{ge}$ (360 mg/min), and then falls up to the zero. The outline of the $G_{empt}(t)$ plot depends on the amount of carbohydrate (Ch) ingestion. Figure 3(a) depicts the triangular form of the $G_{empt}(t)$ in the condition when, Ch ingestion is below the critical value of carbohydrate Ch_{crit} (10.8 gm). The Ch_{crit} can be estimated by the help of equation (5). The $Tasc_{ge}$ and $Tdes_{ge}$ represent the ascending and descending time of the $G_{empt}(t)$ plot. It is described in equation (6). Figure 3(b) depicts the trapezoidal form of the $G_{empt}(t)$ plot in the condition when Ch ingestion is higher than or identical to the Ch_{crit}. In this study, values of $Tasc_{ge}$ and $Tdes_{ge}$ are taken as 30 min. The $T\max_{ge}$ is the time interval in which $G_{empt}(t)$ attains the $V\max_{ge}$. It is stated in the equation (7) (Lehmann, 1992, 1998).

$$Ch_{crit} = \left[\left(Tasc_{ge} + Tdes_{ge}\right) V\max_{ge}\right]/2 \tag{5}$$

$$Tasc_{ge} = Tdes_{ge} = Ch/V\max_{ge} \tag{6}$$

$$\begin{aligned} &T\max_{ge} \\ &= \left[Ch - (1/2)V\max_{ge}\left(Tasc_{ge} + Tdes_{ge}\right)\right]/V\max_{ge} \end{aligned} \tag{7}$$

The $G_{empt}(t)$ with Ch intake higher than Ch_{crit} is characterised as:

$$G_{empt}(t) = \begin{cases} \left(V\max_{ge}/Tasc_{ge}\right) & \text{if } t < Tasc_{ge} \\ V\max_{ge} & \text{if } Tasc_{ge} < t \le Tasc_{ge} + T\max_{ge} \\ V\max_{ge} & \text{if } Tasc_{ge} + T\max_{ge} \le t < Tasc_{ge} + T\max_{ge} + Tdes_{ge} \\ -\left(V\max_{ge}/Tdes_{ge}\right)t & \\ 0 & \text{if otherwise} \end{cases} \tag{8}$$

where t is the interval of the time from the instance of meal ingestion. The $G_{empt}(t)$ plot for both triangular and trapezoidal form can be acknowledged and expected for the calculation purpose by indicating the equation (8). The glucose preoccupation rate from gut is assessed from the 1st order filter production with respect to the input $G_{empt}(t)$ (Lehmann, 1992, 1998).

$$\frac{dG_{gut}(t)}{dt} = G_{empt}(t) - G_{in}(t) \tag{9}$$

$$G_{in}(t) = K_{gabs} G_{gut}(t) \tag{10}$$

where $G_{gut}(t)$ is the gut glucose absorption, $G_{in}(t)$ is the glucose ingestion rate into the VB, K_{gabs} is the gut glucose absorption rate constant, and the value of K_{gabs} is assumed as 0.017 min^{-1}. Figure 3(c) exhibits the glucose assimilation rate from the gut with 10 gm and 60 gm Ch consumption. It is obtained by going of $G_{empt}(t)$ through the 1st order filter and appears in Figures 3(a) and 3(b) separately in both the circumstances. The dynamic conditions as spoken to in equations (5)–(8) for the GES are analysed and executed. Additionally, the dynamic conditions as depicted by the equations (9)–(10) implied for gut are also analysed and executed. The numerical structure of the gut is shown in Figure 4(a).

2.2.3 Profiles of glucose in liver

The liver delivers and uses the carbohydrates, and it is characterised as *NHGB*. The *NHGB* is the glucose profile of the liver, and constrained by two variables as $I_{ep}(t)$ and AG. It is estimated by referring the look-up table. The associated information is collected from the literatures (Lehmann, 1992). The numerical structure of the liver is reflected in Figure 4(a).

2.2.4 Profiles of glucose in cells

The cells utilise glucose dependent on $I_{ea}(t)$ and $I_p(t)$. The glucose utilisation by the cells is synthesised by the look-up table, and the associated information is collected from the literatures (Lehmann, 1992, 1998). The numerical structure of cell is reflected in Figure 4(a).

2.2.5 Profiles of glucose in central nerve system and RBC

The central nerve system (CNS) and RBC are the insulin autonomous organs. CNS and RBC utilise the glucose of 72 mg/hr/kg and 12.96 mg/hr/kg respectively. The numerical structures of the CNS and RBC are reflected in Figure 4(a).

Figure 3 (a) The plot of the $G_{empt}(t)$ with 10 gm *Ch* ingestion ($Ch < Ch_{crit}$) (b) The plot of the $G_{empt}(t)$ with 60 gm *Ch* ingestion ($Ch > Ch_{crit}$) (c) The outcome of the gut with 10 gm and 60 gm *Ch* ingestion (see online version for colours)

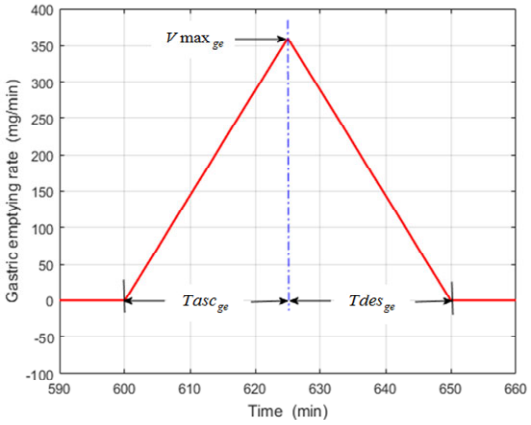

(a)

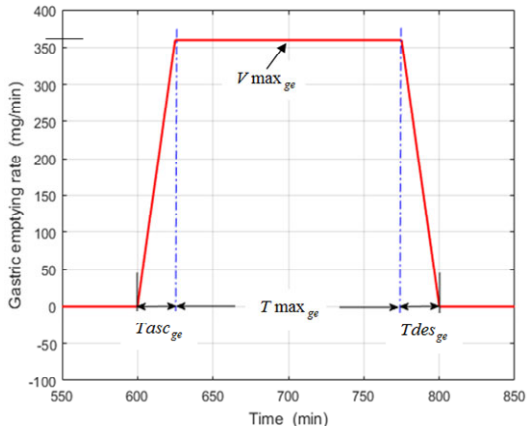

(b)

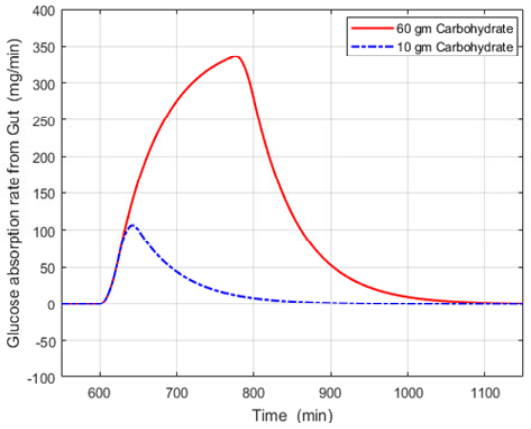

(c)

2.2.6 *Profiles of glucose in kidney*

The kidney eliminates the part of the glucose from the VB, when the BG level ascents up to the *RTG*. The glucose discharge rate of kidney depends upon the BG and creatinine clearance rate (*CCR*). The function of the kidney is stated as follows (Lehmann, 1992, 1998):

$$G_{ren}(t) = CCR\left(G(t) - RTG\right) \text{ if } G(t) > RTG \tag{11}$$

$$G_{ren}(t) = 0 \text{ if } G(t) \le RTG \tag{12}$$

where $G(t)$ and $G_{ren}(t)$ are the BG level (mg/dl) and renal glucose excretion rate respectively. The numerical structure of kidney is illustrated in Figure 4(a). In this study, the *CCR* is identical to 1 dl/min.

2.2.7 *Glucose concentration in VB*

The dynamic equation of BG level in VB is stated as follows (Lehmann, 1992, 1998):

$$\frac{dG(t)}{dt} = \frac{\left[G_{in}(t) + G_{liver}(t) - G_{out}(t) - G_{ren}(t)\right]}{V_G} \tag{13}$$

where V_G, $G_{out}(t)$, and $G_{liver}(t)$ are the glucose distribution volume in the VB, total glucose consumption rate of all GM organs, and *NHGB* rate of the liver separately. In this study, V_G is taken as 175 dl.

2.3 *Mathematical structure of patient*

The structure of the patient is shown in the Figure 4(a). It is formulated regarding to the mathematical expressions as signified in equations (1)–(13).

2.4 *MID*

Cochin (1997) recommends one sort of MID for this study. It works on the principle of variable pumping rate. The most crucial components of this device are the storage capsule, micro pump, accumulator, pump return valve, and proper electrical control. A chromatograph for testing BG levels, an accelerometer for determining if the patient is active or resting, and a pulse monitor for monitoring heart rate are among the other sensing and regulating components. All of this information is gathered by a microprocessor, which then makes the decision to give proper insulin doses to the VB. In Figure 4(b), the MID's simulation structure is shown.

2.5 *Investigation of patient dynamics*

The time domain response fluctuation of numerous parameters associated to BG metabolic processes is demonstrated in this section using a 60.00 gm meal at 600 minutes and exercise at 1,300 minute workout under Gaussian environment. A fixed insulin dose, known as the basal dose of insulin, is used in this study. Figure 5(a) depicts the transitory variations in plasma glucose levels in VB as well as the insulin dose. Figure 5(b) depicts the abnormalities in NHGB rate, gut rate, rate of kidney excretion, as well as glucose uptake by the CNS and cells.

Figure 4 (a) Simulation structure of MID along with patient (b) MID's simulation structure

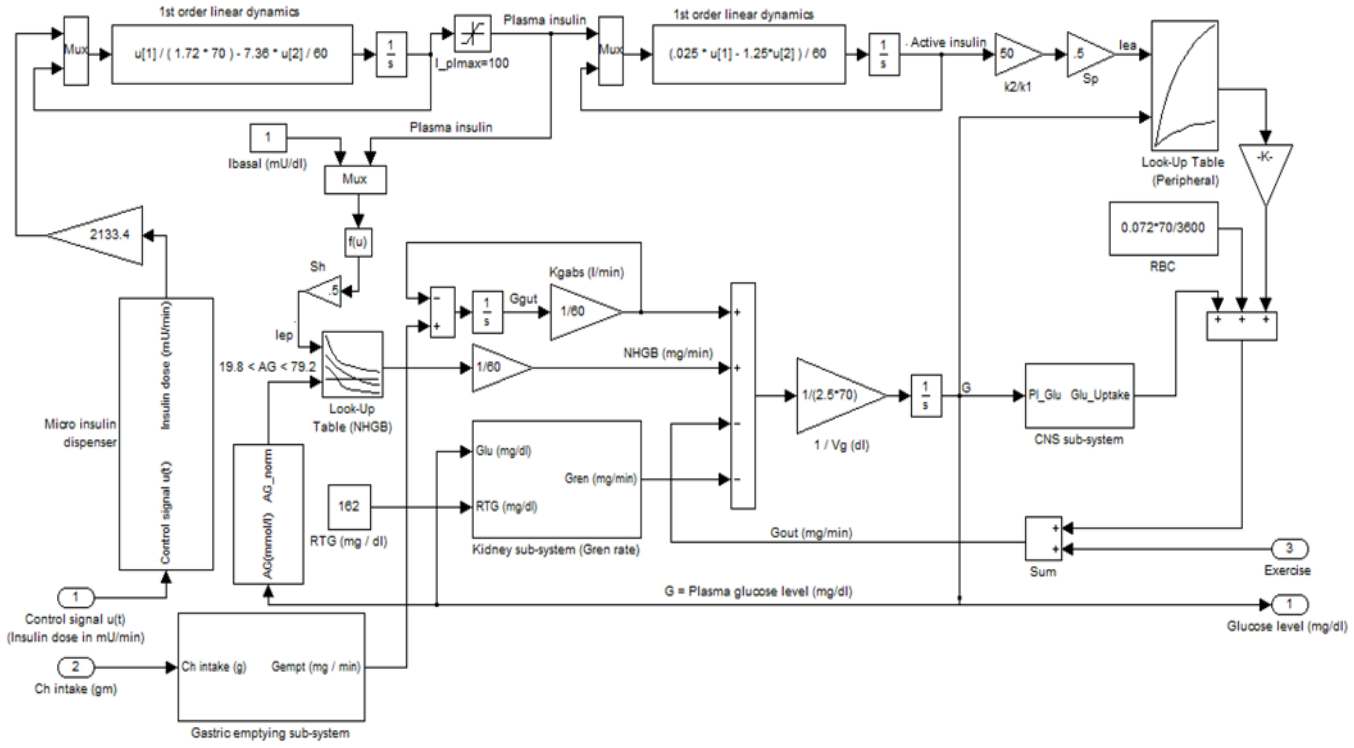

(a)

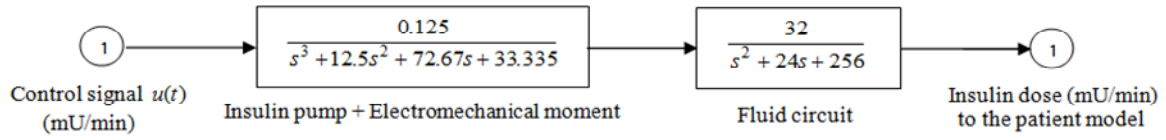

(b)

Peripheral cells and the liver, which rely only on insulin, maintain entire BG control in the VB. The cells and liver consume the least amount of glucose when insulin is not present. In this circumstance, the BG level increases excessively, above the 144 mg/dl target. This leads to the issue of *hyper-glycemia*. The kidney removes part of the glucose from the VB when the BG level reaches the RTG threshold. The rate of glucose excretion by the kidney as a function of BG level is depicted in Figure 5(c). The results in Figures 5(a)–5(c) depict a patient model with a wide range of transient reactions, and the patient's glucose level is always higher than the normal BG level. It shows how sensitive the patient dynamics are to the presence of uncertainty and disturbances. Adaptive control technique-based AP will be designed to overcome these uncertainties and disruptions in the patient model.

3 Control mechanisms

The AOA-VPTIDF control mechanism is clearly established in this section. The patient performance with AOA-VPTIDF controller as far as stability, accuracy and robustness are studied. The control performance indices like settling time in minute t_s (min), steady-state error e_{ss} (%), peak overshoot in mg/dl O_{Peak} (mg/dl), and peak undershoot in mg/dl U_{Peak} (mg/dl) are also assessed and analysed with appropriate justification of the AOA-VPTIDF control activities.

3.1 AOA-VPTIDF controller

The diabetic patient structure with AOA-VPTIDF is reflected in Figure 1. In this control strategy, the error signal $e(t)$ is utilised to generate the control output $u(t)$. The transfer function (TF) of the AOA-VPTIDF controller is defined as (Patra, 2020b; Hashim and Hussain, 2021):

$$TF = \left(K_t \times s^{-n}\right) + \left(\frac{K_i}{s}\right) + K_d\left(\frac{ps}{p+s}\right) \tag{14}$$

where the control parameters are represented by tilt gain (K_t), integral gain (K_i), derivative gain (K_d), coefficient of tilt (n) and pre-filter gain (p). The control parameters are evaluated based on the patient activity for the minimum value of the fitness function like integral time absolute error ($ITAE$) as represented in the equation (15) (Patra, 2020b). The minimum value of fitness function gives better control outcomes such as less settling time along with less overshoot and undershoots.

$$ITAE = \int_0^{\infty} t|e(t)|dt \tag{15}$$

For monitoring of glucose level, control parameters are evaluated by help of the AOA approach.

Figure 5 Patient model (open loop) characteristic curves, (a) BG level verses insulin dose (b) glucose production and utilisation rates of GM organs (c) glucose excretion rate of kidney verses BG level (see online version for colours)

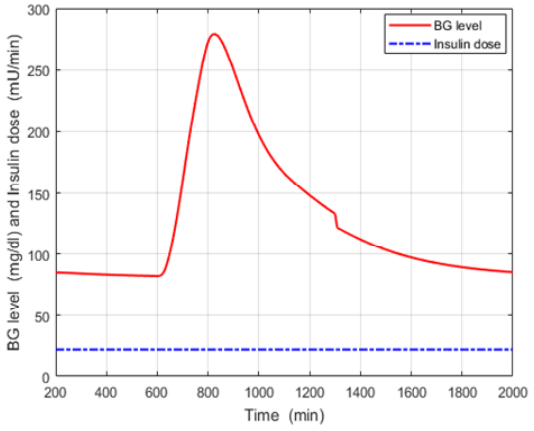

(a)

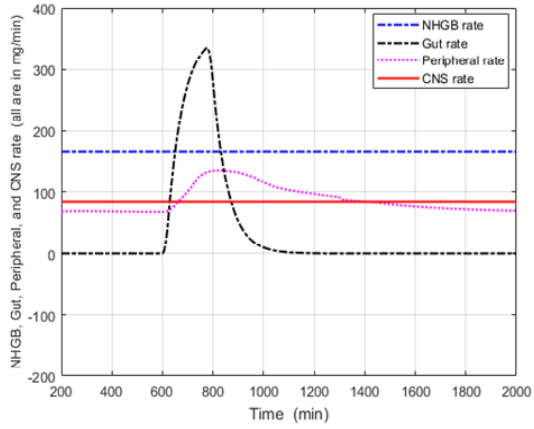

(b)

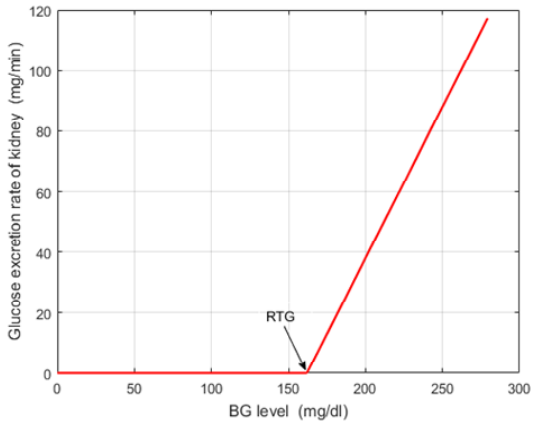

(c)

3.2 Optimisation algorithm

The advent of optimisation algorithms provides better tuning methods. The optimisation algorithms used is Archimedes optimisation (AOA). This is explained in sections appended below.

3.2.1 Archimedes optimisation algorithm

Motivation from AOA is Archimedes law of physics. It is based on the buoyant force exerted by partially or completely immersed in any fluid is proportional to the weight of the displaced liquid (Hashim and Hussain, 2021). AOA is a population based algorithm. It starts with initialisation of total number of iterations, objects, population, optimisation variables, volume, density and acceleration. These values are assigned randomly upon evaluation of its fitness function. The optimisation terminates after evaluating the all iterations. The acceleration of objects is based on the condition of mutual collision of objects. The updated density, volume and acceleration determine new position of the object. It has both exploration and exploitation phase. Hence it is a global optimisation algorithm. Let, N be total number of objects, l_{bi} and u_{bi} be the lower and upper bound of search spaces. The position (o_i) of i^{th} object of the population with N objects is represented by equation (16).

$$o_i = l_{bi} + rand \times (u_{bi} - l_{bi}) \tag{16}$$

where $rand$ is a D dimensional vector that randomly generates number between 0 and 1. The initial value of volume (vol_i) and density (den_i) is expressed by equation (17).

$$\left.\begin{aligned} den_i &= rand \\ vol_i &= rand \end{aligned}\right\} \tag{17}$$

After initialisation the fitness function is evaluated and the object with best fitness value is represented as x_{best}, the best value of volume is vol_{best}, the best value of density is den_{best} and the best value of acceleration is acc_{best}. The updating process of density and volume for current iteration (t) is expressed in equation (18).

$$\left.\begin{aligned} den_i^{t+1} &= den_i^t + rand \times \left(den_{best} - den_i^t\right) \\ vol_i^{t+1} &= vol_i^t + rand \times \left(vol_{best} - vol_i^t\right) \end{aligned}\right\} \tag{18}$$

The objects initially collide mutually and then start to settle around equilibrium point. This is represented by transfer operator (Tf). Tf transforms exploration phase in to exploitation phase. It is represented mathematically by equation (19).

$$Tf = e^{\frac{t - t_{\max}}{t_{\max}}} \tag{19}$$

where $t_{\max}$ is maximum number of iterations. Tf gradually increases from its initial value and settles around one. The transfer from global search to local search is achieved by

density decreasing factor (d). It is expressed mathematically as equation (20).

$$d^{t+1} = e^{\left(\frac{t}{t_{\max}}-1\right)} - \frac{t}{t_{\max}} \tag{20}$$

The values of d^{t+1} decreases with rise in time which aids in convergence. Proper handling of d^{t+1} will help to strike a balance between exploration and exploitation phase. The value of $Tf \leq 0.5$ indicates collision between the objects. The acceleration of i^{th} object for $t + 1$ iteration is updated by selecting a random material (mr) is expressed by equation (21).

$$acc_i^{t+1} = \frac{den_{mr} + vol_{mr} \times acc_{mr}}{den_i^{t+1} \times vol_i^{t+1}} \tag{21}$$

where den_{mr}, vol_{mr} and acc_{mr} represent density, volume and acceleration for the selected random material. The den_i^{t+1} and vol_i^{t+1} represent the density and volume $t + 1$ iteration. The exploitation phase considers no mutual collision between the objects. This phase is implemented by considering $Tf \geq 0.5$. In this phase the acceleration of i^{th} object for $t + 1$ iteration is updated by equation (22).

$$acc_i^{t+1} = \frac{den_{best} + vol_{best} \times acc_{best}}{den_i^{t+1} \times vol_i^{t+1}} \tag{22}$$

where den_{best}, vol_{best} and acc_{best} represent the best values of density, volume and acceleration respectively. Normalisation of acceleration will determine the step size ($acc_{i\sim Norm}^{t+1}$) that each particle will change for achieving optimal solution. It is expressed by equation (23).

$$acc_{i\sim Norm}{}^{t+1} = 0.9 \times \frac{acc_i^{t+1} - \min(acc)}{\max(acc) - \min(acc)} + 0.1 \tag{23}$$

When the object is far away from the optimal solution then the value of acceleration is higher and as the object approaches optimal solution then the acceleration is reduced. The position of i^{th} particle in exploration phase is updated as per equation (24).

$$x_i^{t+1} = x_i^t + 2 \times rand \times acc_{i\sim Norm}{}^{t+1} \times d \times \left(x_{rand} - x_i^t\right) \tag{24}$$

The position of i^{th} particle in exploitation phase is updated as per equation (25).

$$x_i^{t+1} = x_{best}^t + F \times 6 \times rand \times acc_{i\sim Norm}{}^{t+1} \times d \times \left((c_3 \times Tf) \times x_{rand} - x_i^t\right) \tag{25}$$

c_3 and F are constant value and flag employed to change direction of motion of objects. The flag (F) is expressed as per equation (26).

$$L = \begin{cases} +1 & \text{if } (2 \times rand - c_4) \leq 0.5 \\ -1 & \text{if } (2 \times rand - c_4) > 0.5 \end{cases} \tag{26}$$

where c_4 is a constant value. Finally the fitness function is computed and the updated particle position and best values of density, acceleration and volume are recorded. The optimisation is achieved through reduction in cost function or loss function. The optimisation is carried till the limit of objects is reached or the iteration limits is reached. The optimal AOA-VPTIDF control parameters are adopted based on the AOA strategy as mentioned in Table 1. The optimisation (AOA) is achieved through reduction in cost function (*ITAE*). The structure of AOA-VPTIDF is shown in Figure 6(a), which is designed based on the equations (16) to (26). The working principle of the proposed optimisation technique (AOA) is clearly described through a flow chart as shown in Figure 6(b).

Figure 6 (a) Block diagram of AOA-VPTIDF (b) Flowchart of AOA (see online version for colours)

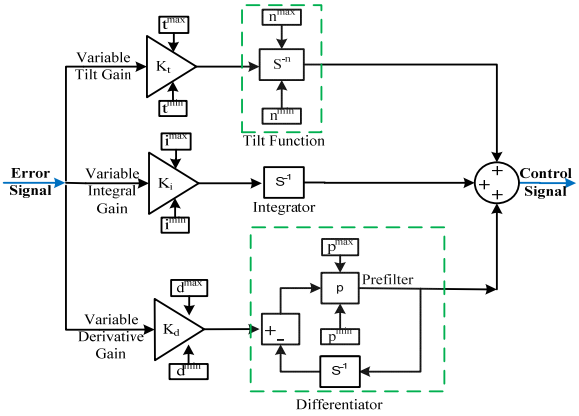

(a)

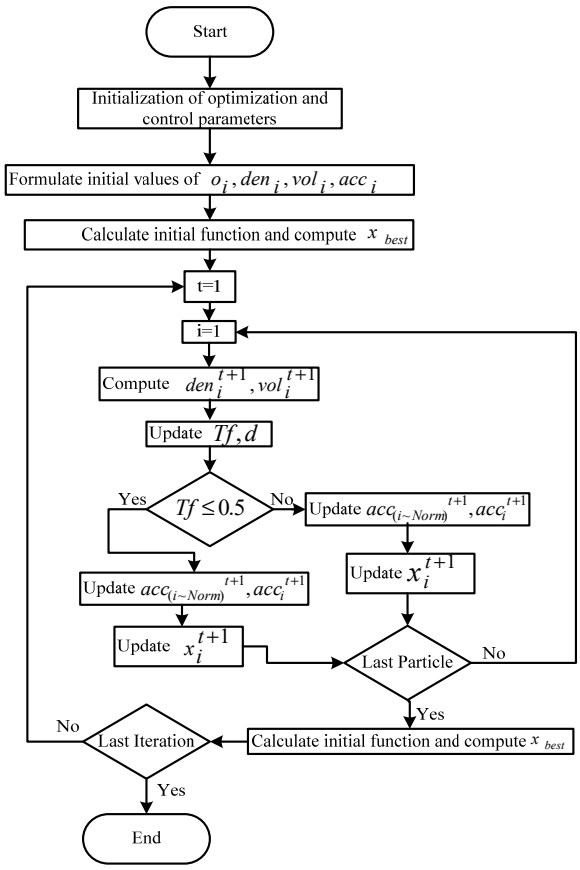

(b)

Table 1 AOA-VPTIDF optimised parameter values

K_t	K_i	K_d	p	n
0.49896	0.003031	0.209	123.5578	0.48456

4 Results and discussion

The BG profiles of the patient model with AOA-VPTIDF controller are analysed thoroughly. The AOA-VPTIDF controller is also compared with the other existing control strategies to validate its enhanced actions.

Figure 7 Patient model (closed loop) characteristic curves, (a) BG level verses insulin dose (b) glucose production and utilisation rates of GM organs (c) glucose excretion rate of kidney verses BG level (see online version for colours)

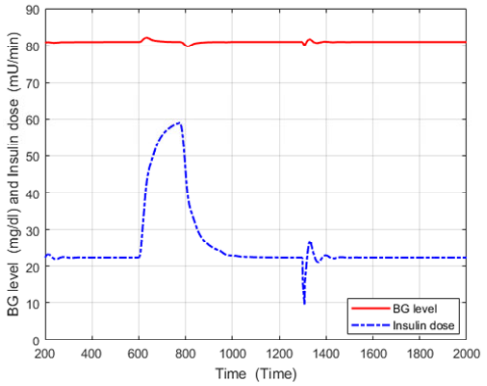

(a)

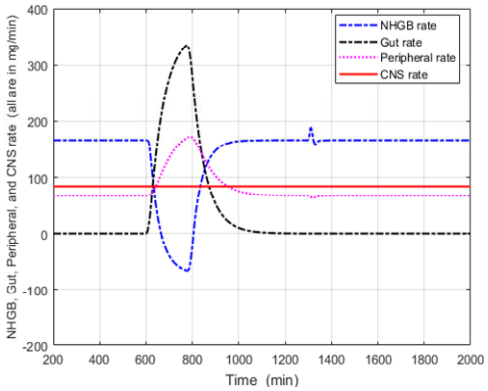

(b)

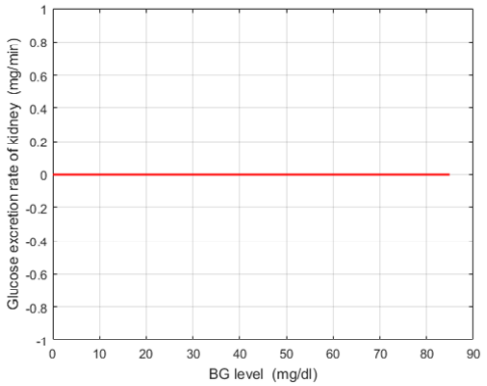

(c)

4.1 *Investigation of patient dynamics with AOA-VPTIDF control*

The AOA-VPTIDF controller for the patient model looked at all of the profiles as well as the related disturbances and uncertainties, such as fluctuating activity, random glucose intake, sensor and actuator noise, and so on. The characteristic curve in-between insulin dose and glucose level are established by eating a 60.00 gm meal at 600 minutes and exercising for 1,300 minutes, as shown in Figure 7(a). Under identical conditions, other profiles such as CNS, NHGB, gut, peripheral and green rates are represented in Figure 7(b).

The response of the patient model with the controller is shown in Figures 7(a)–7(c). In comparison to an uncontrolled process, the data clearly show that insulin-dependent organs including the liver and peripheral cells use more glucose [Figures 5(a)–5(c)]. The BG level drops to 83.3 mg/dl as a result of this impact. So that the problem of *hyper-glycemia* is avoided. Now that the BG level has decreased below the RTG threshold, no additional glucose extraction by the kidney occurs, as shown in Figure 7(c). As a result, the use of the AOA-VPTIDF controller-based AP boosted all patient model characteristics.

4.2 *Robustness aspect of the AOA-VPTIDF controller*

The AOA-VPTIDF controller was put through its paces to prove its worth under two different sets of patient parameters and a wide variety of meal intakes. The BG levels in relation to hepatic and peripheral insulin sensitivity are shown in Figures 8(a) and 8(b). Figure 8(c) shows the BG levels in relation to a wide range of meal consumption. In each case, the BG level reaches 81 mg/dl within a short period of time. As a result, patient features are unaffected by model restrictions or meal intake. It contributes to the AOA-VPTIDF controller's robustness.

Table 2 Comparative investigation with other state of art controllers

Control algorithms	*PID (Sutradhar and Chaudhuri, 2002)*	*Fuzzy (Ibbini, 2006)*	*SM (Patra, 2017a)*	*LQG (Patra, 2015)*	*H_∞ (Patra, 2014)*	*AOA-VPTIDF (proposed)*
Meal intake (gm)	60	60	60	60	60	60
Insulin dose (mU/min)	59.6	59.2	59.0	59.1	59.1	59.0
t_s (min)	290	260	250	260	255	220
O_{Peak} (mg/dl)	5.2	5.3	4.1	8.5	4.5	2.3
U_{Peak} (mg/dl)	3.1	2.1	1.5	1.8	1.2	1.0
Noise (%)	10	10	5	5	5	1
e_{ss} (%)	0	0	0	0	0	0

Figure 8 BG levels of closed loop patient structure verses patient parameters, and meal intakes, (a) BG level verses S_h (b) BG level verses S_p (c) BG level verses meal intakes (see online version for colours)

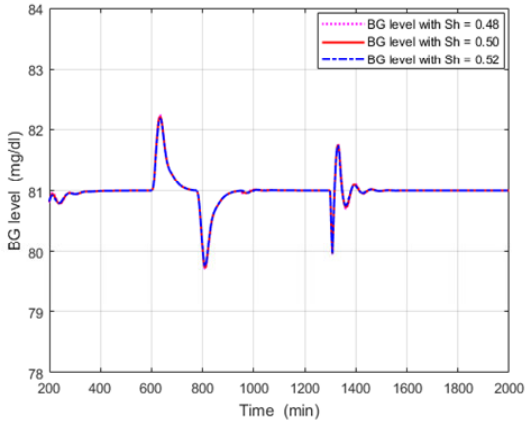

(a)

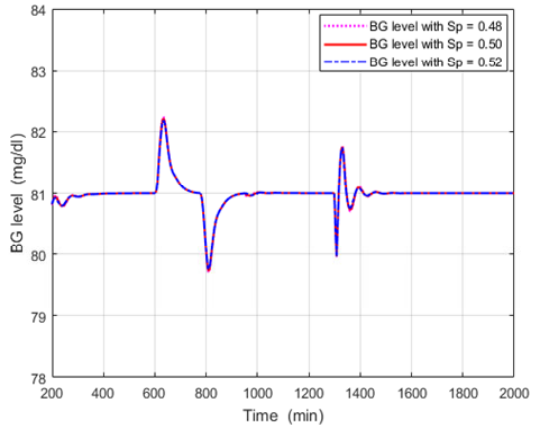

(b)

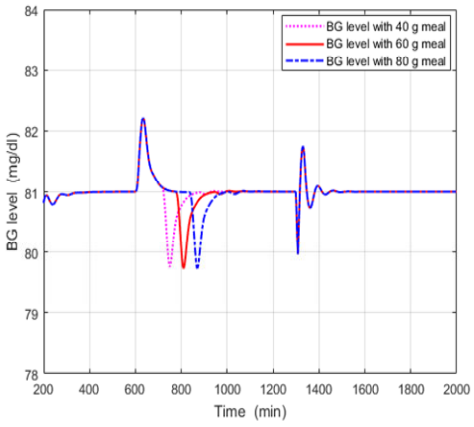

(c)

4.3 *Stability of the patient model*

The bode outputs of an open and closed system are shown in Figures 9(a) and 9(b) to verify that the stability criteria are fulfilled. From the outputs, it can be shown that the closed model [Figure 9(b)] has a greater perfection referring to the more continuous state stability than the opened model [Figure 9(a)]. The bandwidth (BW) of the closed patient model is greater than that of the opened patient model. It clearly demonstrates a faster and more stable dynamics, and the model, in combination with the proposed controller, achieves a glucose level of 81 mg/dl. From, Figure 9(b), it is also seen that both gain and phase margin are positive. Hence, it confirms that the patient's structure, in conjunction with the controller, achieves increased stability.

Figure 9 (a) The frequency response of patient structure (b) The frequency response of patient structure along with AOA-VPTIDF controller (see online version for colours)

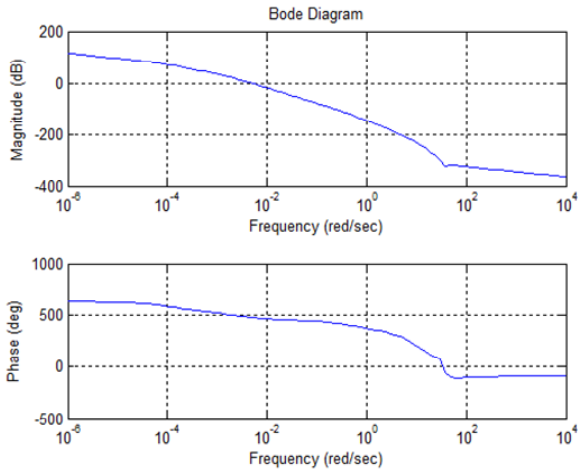

(a)

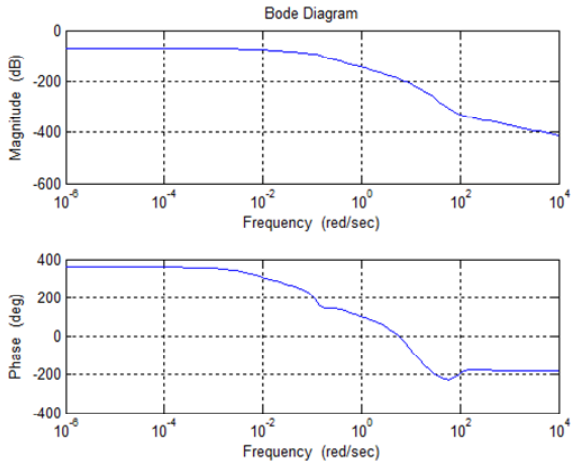

(b)

4.4 *Comparative investigation*

In this part, the control performance of AOA-VPTIDF is compared to that of other control techniques. In diabetic patients employing this controller, the effects of exercise and meal disruption on BG levels and insulin infusion rate changes are depicted in Figures 7(a)–7(c), and Table 2 offers some significant data.

The selected controller's settling time, undershoot, and overshoot are comparatively bigger stability and controllability than other implemented optimum controllers based on patient BG levels with the suggested controller and a 60.00 gm ingested meal disruption.

According to an exercise disturbance test, the AOA-VPTIDF regulated BG level declines to 80.00 mg/dl and is within the *normo-glycemic* range. According to the findings, the AOA-VPTIDF controller performs significantly better and more consistently in minimising noise and resolving *hyper-glycemia* issues. This controller regulates blood sugar levels and reduces insulin infusion rates better than other commonly used controllers. Using an AOA-VPTIDF based controller, the results demonstrated greater reliability, stability, precision, and robust performance in a variety of physiological circumstances and disturbances.

5 Conclusions

This study provides a new control strategy (AOA-VPTIDF) for maintaining BG level in TIDM diabetes patients in the *normo-glycemic* range. For testing and simulation purposes, a patient model with MID has been taken and detailed mathematical representation and Simulink model design has been offered. All of the calculations were done with a variety of uncertainties and disturbances related with food and exercise, all of which were centred on a normal human operating point. The study was carried out with different meal and activity-related uncertainties and disturbances, with a starting operating point set by a normal human body reference with a plasma glucose level of 81 mg/dl and a 22.3 mU/min 'base dose' of insulin. When comparing the suggested control algorithm to the other control methods, it is clear that the proposed control algorithm is more accurate, steady and robust in controlling the BG level. The results suggest that employing an integrated embedded system and other auxiliary devices for BG control in TIDM patients, such as a MID and a sensor, this sort of control approach may be implemented in real-time. However, according to the current state of the system, the tuning approach to identify the best gain is largely dependent on the parameters linked with the technique. In the same stage and state of the control approach, this could be vulnerable. With the aforementioned problems in mind, future research may be conducted to create a more robust, dependable, and effective controller for this situation.

References

Barger, M. and Rodbard, D. (1989) 'Computer simulation of plasma insulin and glucose dynamics after subcutaneous insulin injection', *Diabetes Care*, Vol. 12, No. 1, pp.725–736.

Chee, F. and Andrey, V. (2005) 'Optimal H_∞ insulin injection control for blood glucose regulation in diabetic patients', *IEEE Trans. Biomed. Eng.*, Vol. 52, No. 10, pp.1625–1631.

Chee, F. and Fernando, T. (2003) 'Closed-loop glucose control in critically ill patients using continuous glucose monitoring system (CGMS) in real time', *IEEE Transactions on Information Technology in Biomedicine*, Vol. 7, No. 4, pp.43–53.

Cochin, L. (1997) *Analysis and Design of Dynamic Systems*, 3rd ed., Addison-Wesley, New York.

Frederick, C. and Tyrone, L. (2003) 'Expert PID control system for blood glucose control in critically ill patients. Information technology in biomedicine', *IEEE Transactions*, Vol. 7, No. 4, pp.419–425.

Gallardo, H. and Ana, G. (2013) 'High-order sliding-mode control for blood glucose: practical relative degree approach', *Control Engineering Practice*, Vol. 21, No. 5, pp.747–758.

Hashim, F.A. and Hussain, K. (2021) 'Archimedes optimization algorithm: a new metaheuristic algorithm for solving optimization problems', *Applied Intelligence*, Vol. 51, No. 3, pp.1531–1551.

Ibbini, M. (2006) 'The PI-fuzzy logic controller for the regulation of blood glucose level in diabetic patients', *Journal of Medical Engineering and Technology*, Vol. 30, No. 2, pp.83–92.

Kamath, S. and George, V.I. (2009) 'Simulation study on closed loop control algorithm of type 1 diabetes mellitus patients', *IETE Journal of Research*, Vol. 55, No. 1, pp.230–235.

Karimpour, A. (2012) 'Knowledge-based closed-loop control of blood glucose concentration in diabetic patients and comparison with H_∞ control technique', *IETE Journal of Research*, Vol. 58, No. 1, pp.328–336.

Lehmann, E.D. (1992) 'Physiological model of glucose-insulin interaction in type-1 diabetes mellitus', *Journal of Biomedical Engineering*, Vol. 14, No. 3, pp.235–242.

Lehmann, E.D. (1998) 'Compartmental models for glycaemic prediction and decision support in clinical diabetes care: promise and reality', *Computer Methods and Programs in Biomedicine*, Vol. 56, No. 1, pp.193–204.

Patra, A.K. (2014) 'Optimal H-infinity insulin injection control for blood glucose regulation in IDDM patient using physiological model', *Int. J. Automation and Control*, Vol. 8, No. 4, pp.309–322.

Patra, A.K. (2015) 'An automatic insulin infusion system based on LQG control technique', *Int. J. Biomedical Engineering and Technology*, Vol. 17, No. 3, pp.252–275.

Patra, A.K. (2017a) 'Adaptive sliding mode Gaussian controller for artificial pancreas in TIDM patient', *J. Process Control*, Vol. 58, No. 1, pp.23–27.

Patra, A.K. (2017b) 'Adaptive continuous-time model predictive controller for implantable insulin delivery system in type I diabetic patient', *Optimal Control Applications and Methods*, Vol. 38, No. 2, pp.184–204.

Patra, A.K. (2018a) 'Backstepping sliding mode Gaussian insulin injection control for blood glucose regulation in TIDM patient', *J. Dyn. Sys. Meas. Control*, Vol. 140, No. 9, pp.091006–091006-15.

Patra, A.K. (2018b) 'Backstepping model predictive controller for blood glucose regulation in type-I diabetes patient', *IETE Journal of Research*, Vol. 66, No. 3, pp.326–340.

Patra, A.K. (2020a) 'Design of artificial pancreas based on the SMGC and self-tuning PI control in type-I diabetic patient', *International Journal of Biomedical Engineering and Technology*, Vol. 32, No. 1, pp.1–35.

Patra, A.K. (2020b) 'The fractional order PID controller design for BG control in type-I diabetes patient', *Advances in Intelligent Computing and Communication*, pp.321–329, Springer, Singapore.

Patra, A.K. (2020c) 'Design of artificial pancreas based on fuzzy logic control in type-I diabetes patient', *Innovation in Electrical Power Engineering, Communication, and Computing Technology*, pp.557–569, Springer, Singapore.

Patra, A.K. (2020d) 'Design of backstepping LQG controller for blood glucose regulation in type I diabetes patient', *International Journal of Automation and Control*, Vol. 14, No. 4, pp.445–468.

Patra, A.K. (2020e) 'Kalman filtering linear quadratic regulator for artificial pancreas in type-I diabetes patient', *International Journal of Modelling, Identification and Control*, Vol. 34, No. 1, pp.59–74.

Rmileh, A. and Gabin, W. (2012) 'Wiener sliding-mode control for artificial pancreas: a new nonlinear approach to glucose regulation', *Computer Methods and Programs in Biomedicine*, Vol. 107, No. 1, pp.327–340.

Sutradhar, A. and Chaudhuri, S. (2002) 'Analysis and design of an optimal PID controller for insulin dispenser system', *Journal of Institution of Engineers (India)*, Vol. 82, No. 2, pp.304–313.